Supplementary Figure 1

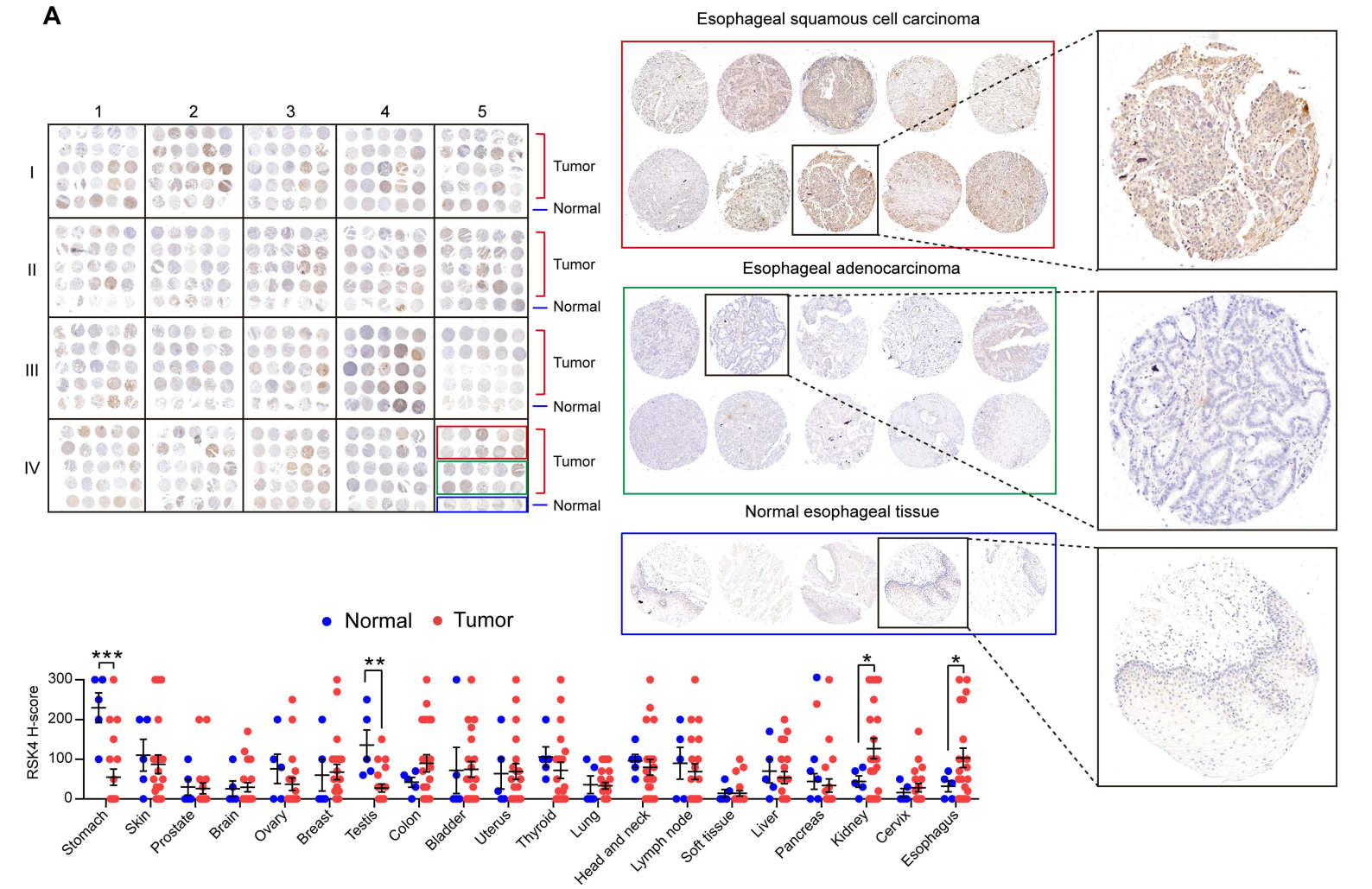

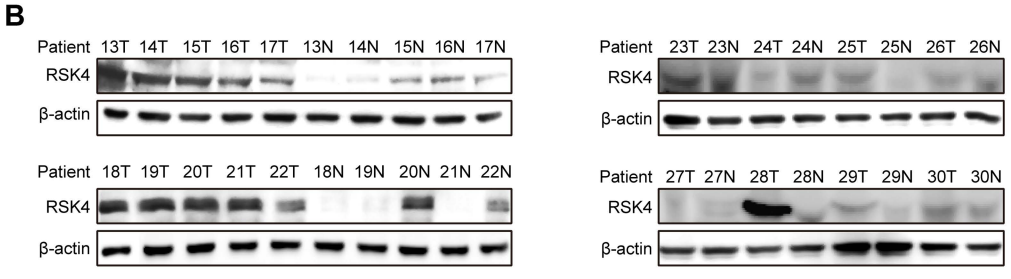

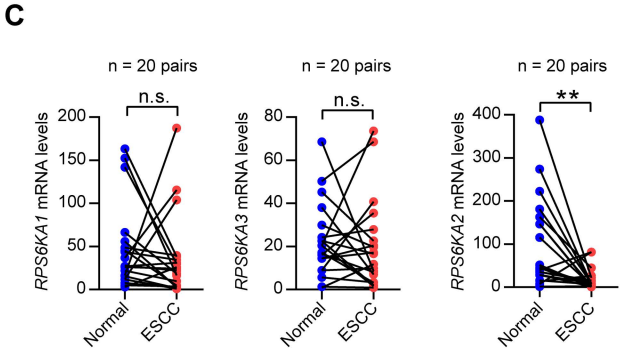

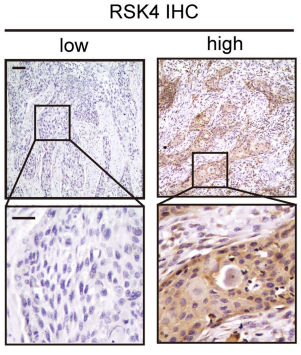

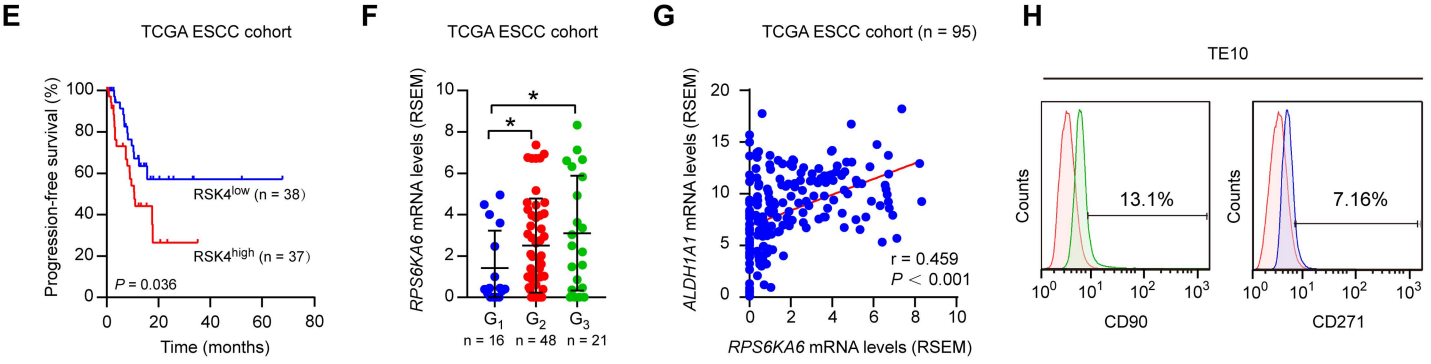

Supplementary Figure 1. RSK4 is highly expressed in ESCC CSCs. (A) RSK4 protein H-score of tissue microarray across 20 kinds of human tumors and corresponding normal tissues detected by immunohistochemistry (IHC). Representative IHC staining images of RSK4 in ESCC, esophageal adenocarcinoma and normal esophageal tissues were showed. Detailed information of tumor types is presented in **Supplementary Table 1**. (B) Representative western blot analysis of RSK4 expression in ESCC tumor tissues (T) and adjacent non-tumor tissues (N). Protein expression was normalized to β-actin levels. (C) The mRNA levels of *RPS6KA1*, *RPS6KA3* and *RPS6KA2* in 20 pairs of ESCC samples and adjacent non-tumor tissues were determined by real-time PCR. *GAPDH* was used as a loading control. (D) Representative IHC staining with high and low RSK4 protein expression. Scale bars, 100 μm. The median RSK4 IHC H-score was used as the cut-off to distinguish between high and low protein expression. (E) Kaplan-Meier estimation of the ESCC progression-free survival time based on the RSK4 expression levels in the Cancer Genome Atlas (TCGA) cohort. (F) *RPS6KA6* mRNA was overexpressed in Grade 2 (G_2) and Grade 3 (G_3) ESCC cases compared with Grade 1 (G_1) cases from the TCGA ESCC cohort. (G) Correlation between the *RPS6KA6* and *ALDH1A1* mRNA expression patterns in The Cancer Genome Atlas (TCGA) dataset. (H) Flow cytometry analysis of the proportion of $CD90^+$ and $CD271^+$ subpopulations in TE10 cells. ESCC, esophageal squamous cell carcinoma. n.s., not significant. Data are representative of means ± SD. $*P < 0.05$, $**P < 0.01$, $***P < 0.001$. Differences were tested using paired (C) and unpaired (A) 2-sided Student's t test, 1-way ANOVA with Tukey's post hoc test (F) and Log-rank test (E). The correlation was determined by Pearson's correlation test (G).

Supplementary Figure 2

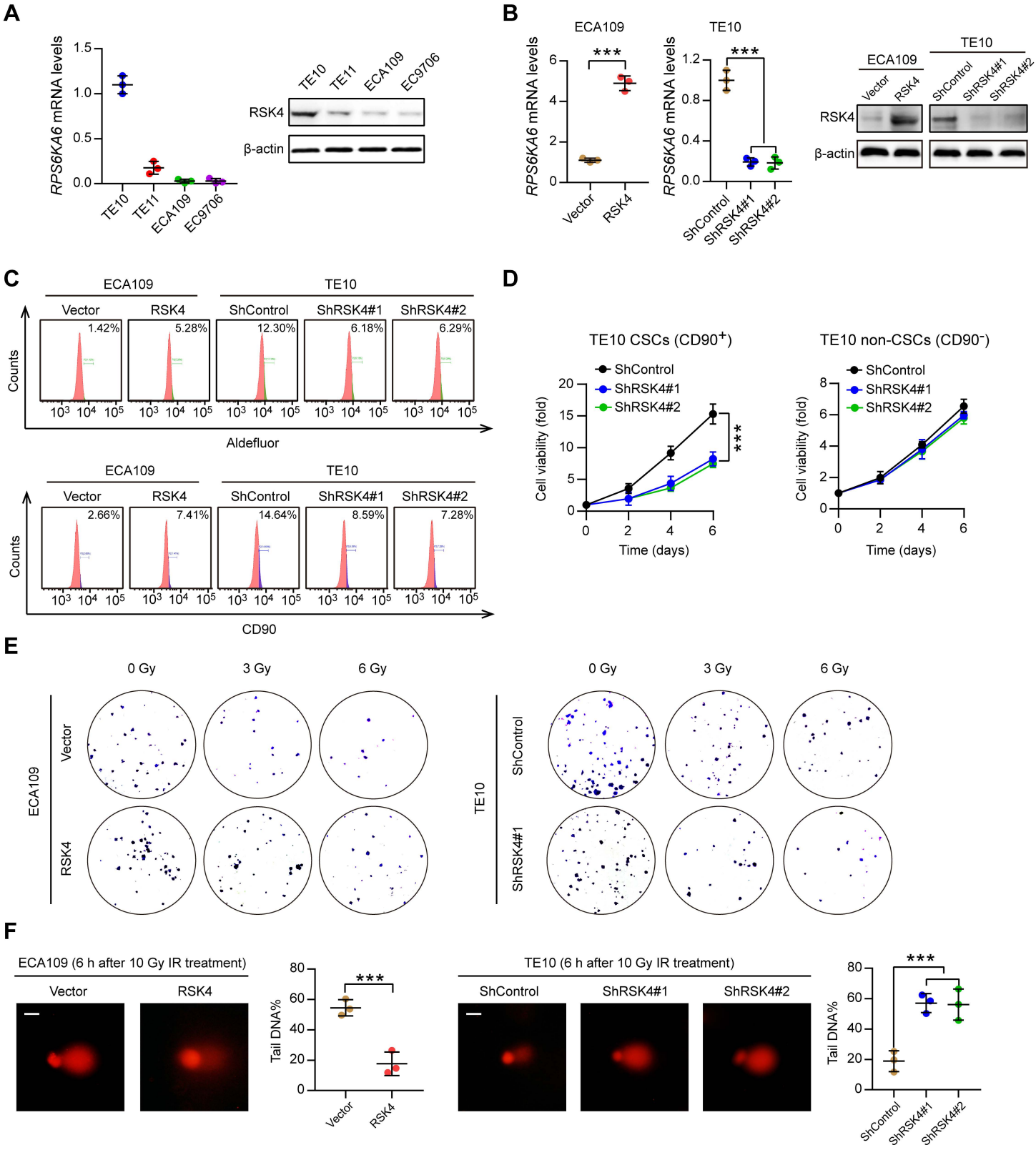

Supplementary Figure 2. Effects of RSK4 on the CSC properties and radioresistance of ESCC cells. (A) Real-time PCR (n = 3 independent experiments) and western blot analysis of RSK4 expression in TE10, TE11, ECA109 and EC9706 cells. (B) Real-time PCR (n = 3 independent experiments) and western blot assays were used to detect the mRNA and protein levels of RSK4 in ESCC cells infected with RSK4 overexpression lentivirus and the knockdown efficiency of RSK4 using shRNA in ESCC cells. (C) Flow cytometry analysis of ALDH activity and the proportion of $CD90^+$ cells in ESCC cells with overexpression or knockdown of RSK4. (D) Effects of RSK4 knockdown on the cell viability of the TE10 CSCs ($CD90^+$ subpopulations) and matched TE10 non-CSCs ($CD90^-$ subpopulations) (n = 3 independent experiments). (E) Representative images of clonogenic assays of ESCC cells with overexpression or knockdown of RSK4 at the indicated irradiation doses. (F) ESCC cells from the indicated groups were treated with IR (10 Gy) and recultured under normal conditions for 6 h, and then subjected to comet assay analysis (n = 3 independent experiments). Scale bars, 100 μm. Data are representative of means ± SD. ***$P < 0.001$. Differences were tested using 1-way ANOVA with Tukey's post hoc test (A, B, D, F).

Supplementary Figure 3

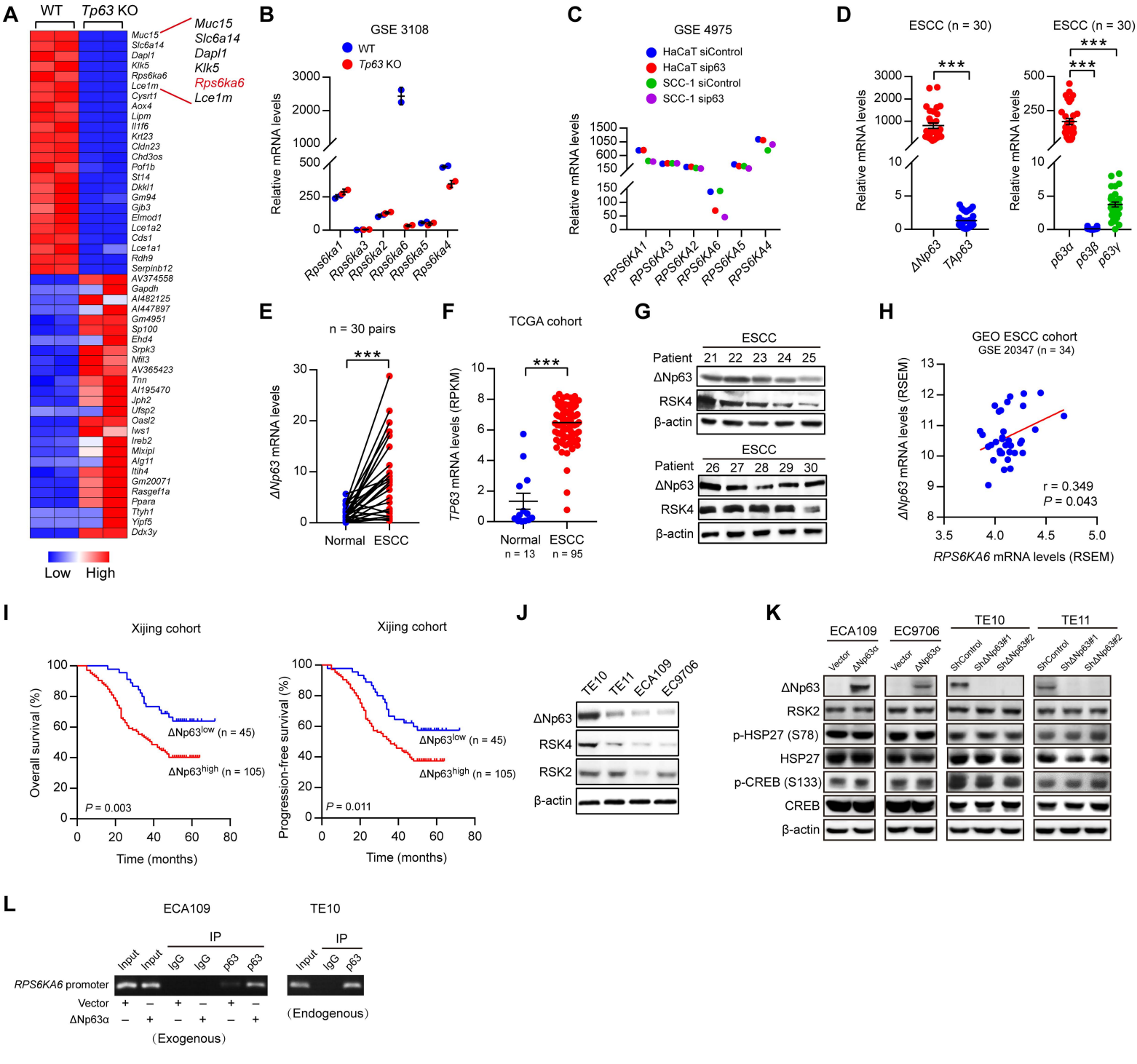

Supplementary Figure 3. RSK4 is a direct transcriptional target of ΔNp63α. (A) Heatmaps showing the top and bottom 50 most differentially expressed genes in E18.5 wild-type (WT) or *Tp63* null mice squamous epithelia (GEO: GSE3108). (B) mRNA levels of *Rps6ka1*, *Rps6ka3*, *Rps6ka2*, *Rps6ka6*, *Rps6ka5* and *Rps6ka4* in E18.5 WT or *Tp63* null mice squamous epithelia (GEO: GSE3108). (C) mRNA levels of *RPS6KA1*, *RPS6KA3*, *RPS6KA2*, *RPS6KA6*, *RPS6KA5* and *RPS6KA4* in the human keratinocyte cell line HaCaT and squamous cell carcinoma cell line SCC-1 with p63 knockdown (GEO: GSE 4975). (D) Real-time PCR analysis of the *p63α*, *p63β*, *p63γ*, *ΔNp63*, and *TAp63* mRNA levels in 30 ESCC tissues. (E) mRNA levels of *ΔNp63* in 30 pairs of ESCC samples and adjacent non-tumor tissues were determined by real-time PCR. *GAPDH* was used as a loading control. (F) *TP63* mRNA expression is upregulated in ESCC compared with normal esophagus tissue from the Cancer Genome Atlas (TCGA) dataset. (G) Expression of ΔNp63 and RSK4 were detected by western blot. (H) Correlation between *RPS6KA6* and *ΔNp63* mRNA expression in 34 ESCC patients from GSE 20347. (I) Kaplan-Meier estimation of ESCC overall survival (left) and progression-free survival (right) based on the ΔNp63 expression levels in the Xijing cohort. (J) Immunoblot analyses of ΔNp63, RSK4, and RSK2 in TE10, TE11, ECA109 and EC9706 cells. (K) Immunoblot analyses of ΔNp63, RSK2, p-HSP27 (S78), HSP27, p-CREB (S133), and CREB in ESCC cells with overexpression or knockdown of ΔNp63. (L) Chromatin immunoprecipitation analysis of the interaction between ΔNp63 and RSK4 in ECA109 cells (left) and TE10 ESCC cells (right). Data are representative of means ± SD. ***$P < 0.001$. Differences were tested using paired (E) and unpaired (F) 2-sided Student's t test, 1-way ANOVA with Tukey's post hoc test (D) and Log-rank test (I). The correlation was determined by Pearson's correlation test (H).

Supplementary Figure 4

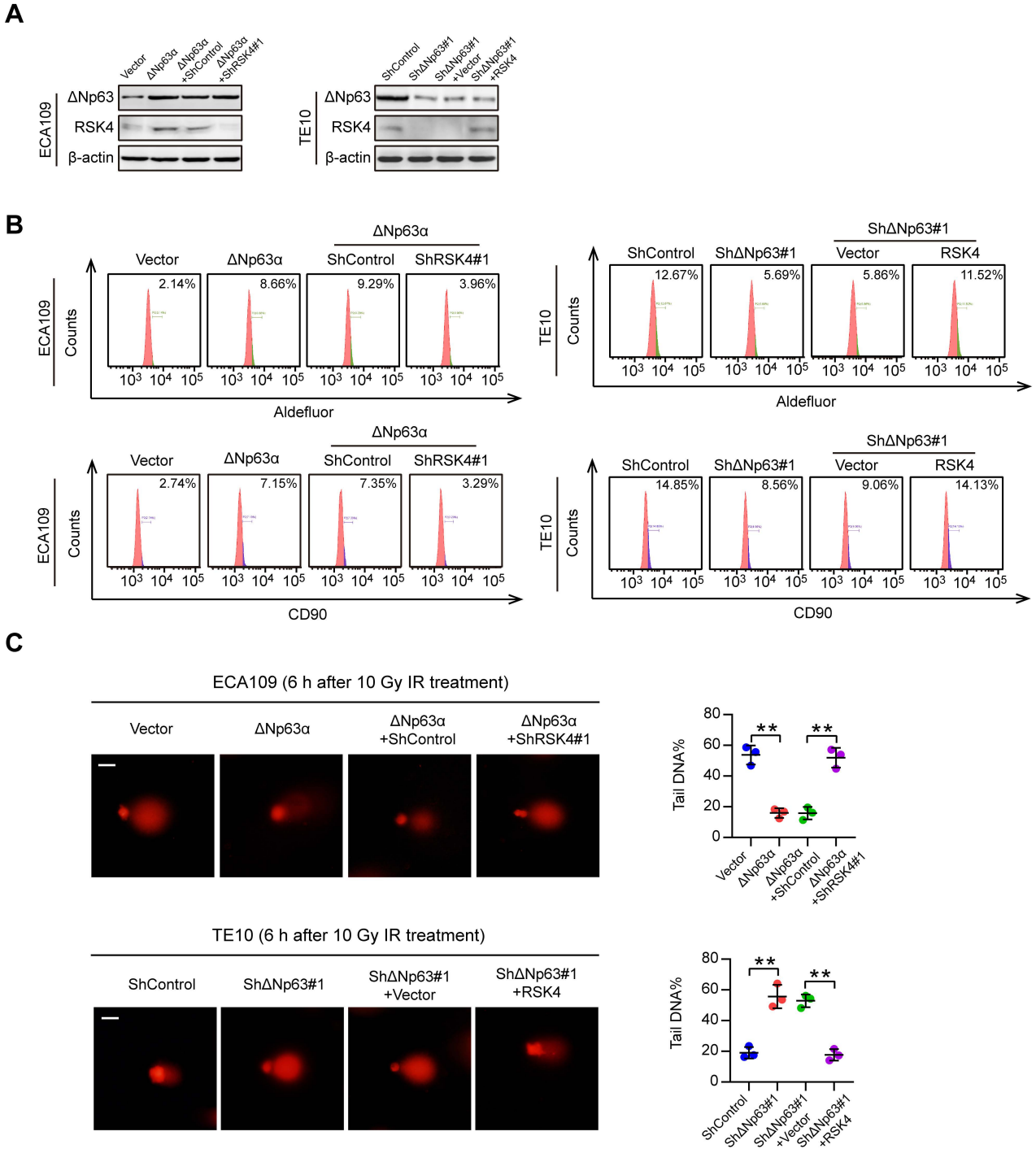

Supplementary Figure 4. RSK4 is essential for the ΔNp63α-mediated CSC properties and radioresistance of ESCC. (A) After stably knocking down RSK4 in ΔNp63α-overexpressing ECA109 cells, protein expression of ΔNp63 and RSK4 was detected by western blot. After stably overexpressing RSK4 in ΔNp63-suppressing TE10 cells, protein expression of ΔNp63 and RSK4 was detected by western blot. (B) Flow cytometry analysis of ALDH activity and the proportion of $CD90^+$ cells in ESCC cells from the indicated groups. (C) ESCC cells from the indicated groups were treated with IR (10 Gy) and recultured under normal conditions for 6 h, and then subjected to comet assay analysis (n = 3 independent experiments). Scale bars, 100 μm. Data are representative of means ± SD. $^{**}P < 0.01$. Differences were tested using 1-way ANOVA with Tukey's post hoc test (C).

Supplementary Figure 5

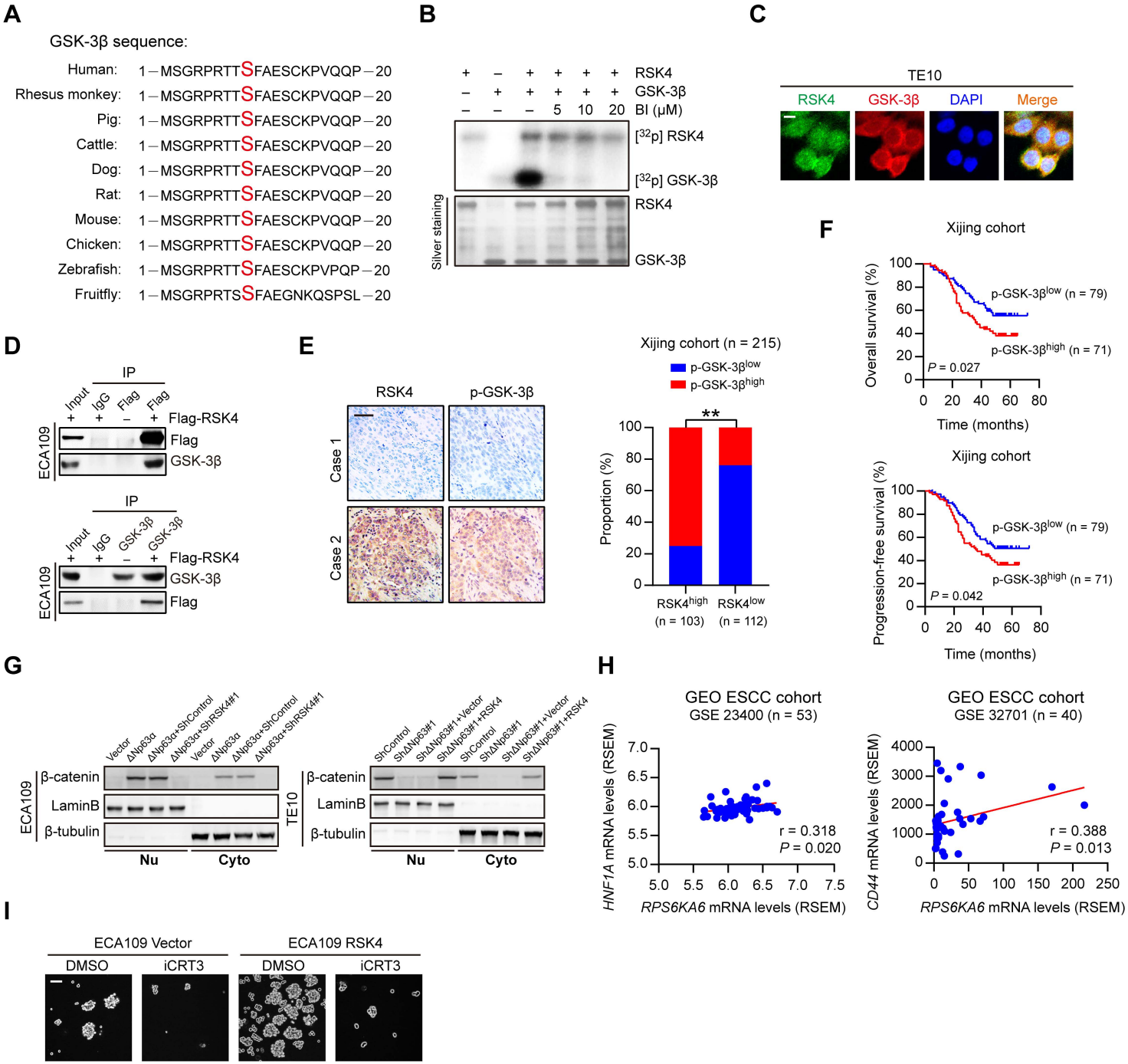

Supplementary Figure 5. RSK4 activates the β-catenin signaling pathway by phosphorylating GSK-3β Ser9. (A) Alignment analysis identified that Ser9 of GSK-3β was highly conserved from fruit fly to human. (B) In vitro kinase assay indicating that the phosphorylation level of GSK-3β was inhibited when treated with BI-D1870 for 2 h. The input was confirmed by silver staining. (C) Colocalization of RSK4 and GSK-3β was visualized by confocal microscopy in TE10 cells. Scale bars, 100 μm. (D) Western blot showing that exogenous RSK4 coimmunoprecipitates (IP) with GSK-3β in ECA109 cells. FLAG-tagged RSK4 or the control vector was transfected. An anti-FLAG antibody could not IP GSK-3β and an anti-GSK-3β antibody could not IP RSK4 in the absence of tagged RSK4. (E) Representative immunohistochemical (IHC) staining images of RSK4 and p-GSK-3β protein expression in ESCC patients from the Xijing cohort. Scale bars, 100 μm. Histograms showing the correlation of IHC data for high or low RSK4 expression relative to the level of p-GSK-3β. (F) Kaplan-Meier estimation of ESCC overall survival and progression-free survival based on p-GSK-3β expression levels in the Xijing cohort. The median p-GSK-3β IHC H-score was used as the cut-off to distinguish between high and low protein expression. (G) Knockdown of RSK4 decreased the protein level of cytoplasmic and nuclear β-catenin in ΔNp63α-overexpressing ESCC cells, whereas overexpression of RSK4 increased the protein level of cytoplasmic and nuclear β-catenin in ΔNp63-suppressing ESCC cells. (H) The correlation between *RPS6KA6* and the Wnt/β-catenin pathway downstream targets *HNF1A* and *CD44* mRNA according to the expression patterns from GSE 23400 and GSE 32701. (I) Representative images of tumor spheres of control or RSK4-overexpressing ECA109 cells treated with iCRT3 (an inhibitor of β-catenin signaling; 50 μM) for 24 h. Scale bars, 50 μm. Nu, nucleus; Cyto, cytoplasm. Data are representative of means ± SD. $^{**}P < 0.01$. Differences were tested using Chi-square test (E) and Log-rank test (F). The correlation was determined by Pearson's correlation test (H).

Supplementary Figure 6

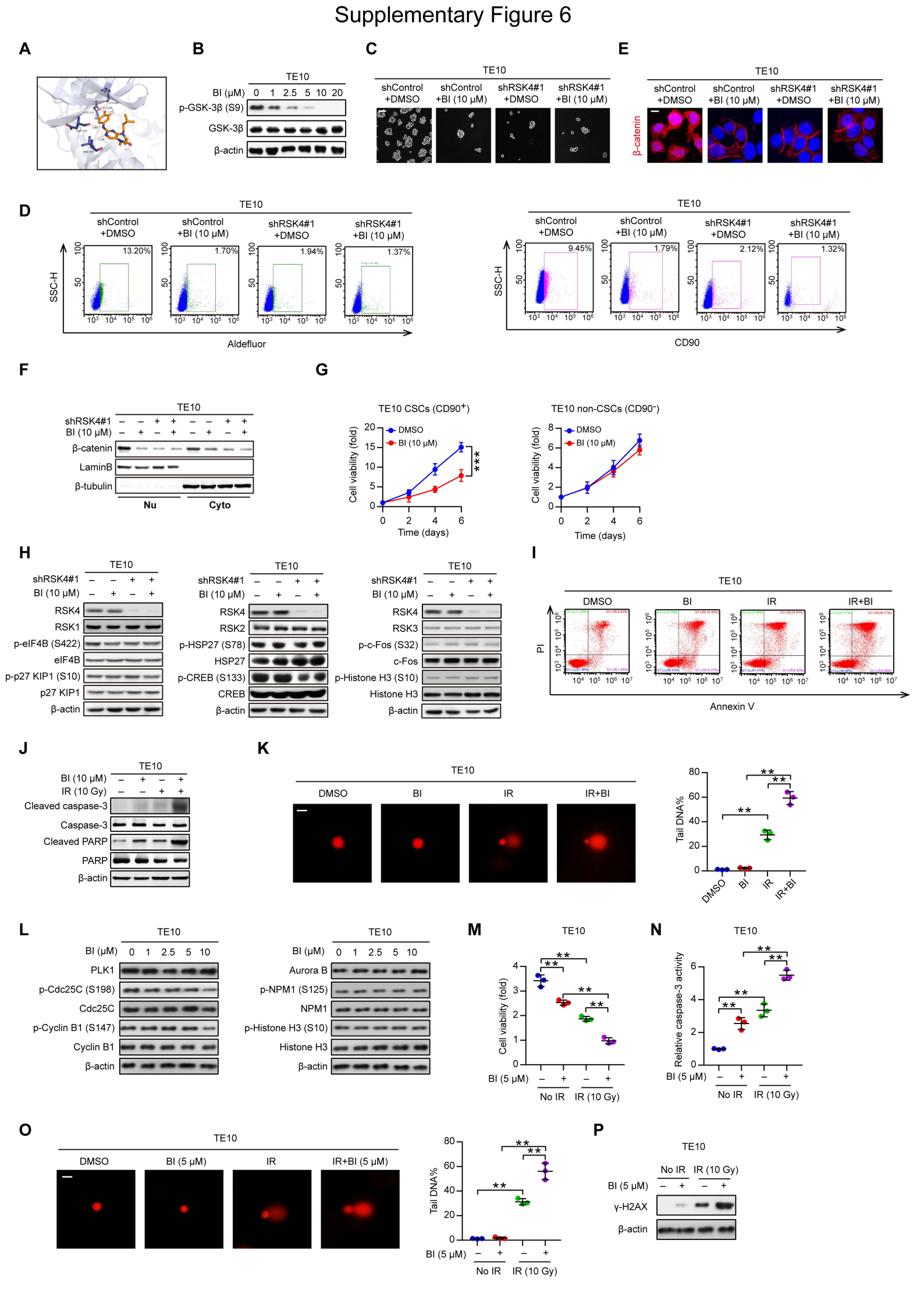

Supplementary Figure 6. Disrupting the RSK4 pathway reduces the CSC properties and improves the radiosensitivity of ESCC. (A) The predicted binding mode of BI-D1870 at the ATP-binding site of the RSK4 N-terminal kinase domain (NTKD). The RSK4 NTKD protein is shown as a cartoon in light purple with transparency, and the ligand is depicted as orange sticks. Important residues are shown as green sticks. Hydrogen bonds are shown as red dashed lines. (B) Immunoblot analyses of p-GSK-3β in TE10 cells treated with the indicated doses of BI-D1870 or the vehicle control. (C) Representative images of tumor spheres of TE10 cells treated with BI-D1870 (10 μM), RSK4 knockdown or both. Scale bars, 100 μm. (D) Flow cytometry analysis of ALDH activity and the proportion of $CD90^+$ cells of TE10 cells with the indicated treatments. (E) Immunofluorescent staining of β-catenin nuclear localization in TE10 cells with the indicated treatments. Scale bars, 100 μm. (F) Immunoblot analyses of the levels of cytoplasmic and nuclear β-catenin in TE10 cells with the indicated treatments. (G) Effects of BI-D1870 treatment (10 μM) on the cell viability of the TE10 CSCs ($CD90^+$ subpopulations) and matched TE10 non-CSCs ($CD90^-$ subpopulations) (n = 3 independent experiments). (H) Immunoblot analyses of RSK1-3 proteins and the phosphorylation levels of their downstream substrates in TE10 cells with the indicated treatments. (I) Cell apoptosis analyses of TE10 cells treated with BI-D1870 (10 μM) for 12 h, IR (10 Gy) or both. (J) Immunoblot analyses of cleaved caspase-3, caspase-3, cleaved PARP and PARP in TE10 cells with the indicated treatments. (K) TE10 cells were treated with BI-D1870 (10 μM) for 12 h, IR (10 Gy) or both and recultured under normal conditions for 6 h, and then subjected to comet assay analysis (n = 3 independent experiments). Scale bars, 100 μm. (L) Immunoblot analyses of PLK1 and Aurora B proteins and the phosphorylation levels of their downstream substrates in TE10 cells with the indicated treatments. (M) Cell viability assay of TE10 cells with the indicated treatments (n = 3 independent experiments). (N) Relative caspase-3 activity in TE10 cells with the indicated treatments (n = 3 independent experiments). (O, P) TE10 cells were treated with BI-D1870 (5 μM) for 12 h, IR (10 Gy) or both and recultured under normal conditions for 6 h, and then subjected to comet assay analysis (O) (n = 3 independent experiments) and Western blot analysis with γ-H2AX antibody (P). Scale bars, 100 μm. Nu, nucleus; Cyto, cytoplasm. Data are representative of means ± SD. $^{**}P < 0.01$, $^{***}P < 0.001$. Differences were tested using unpaired 2-sided Student's t test (G) and 1-way ANOVA with Tukey's post hoc test (K, M, N, O).

Supplementary Figure 7

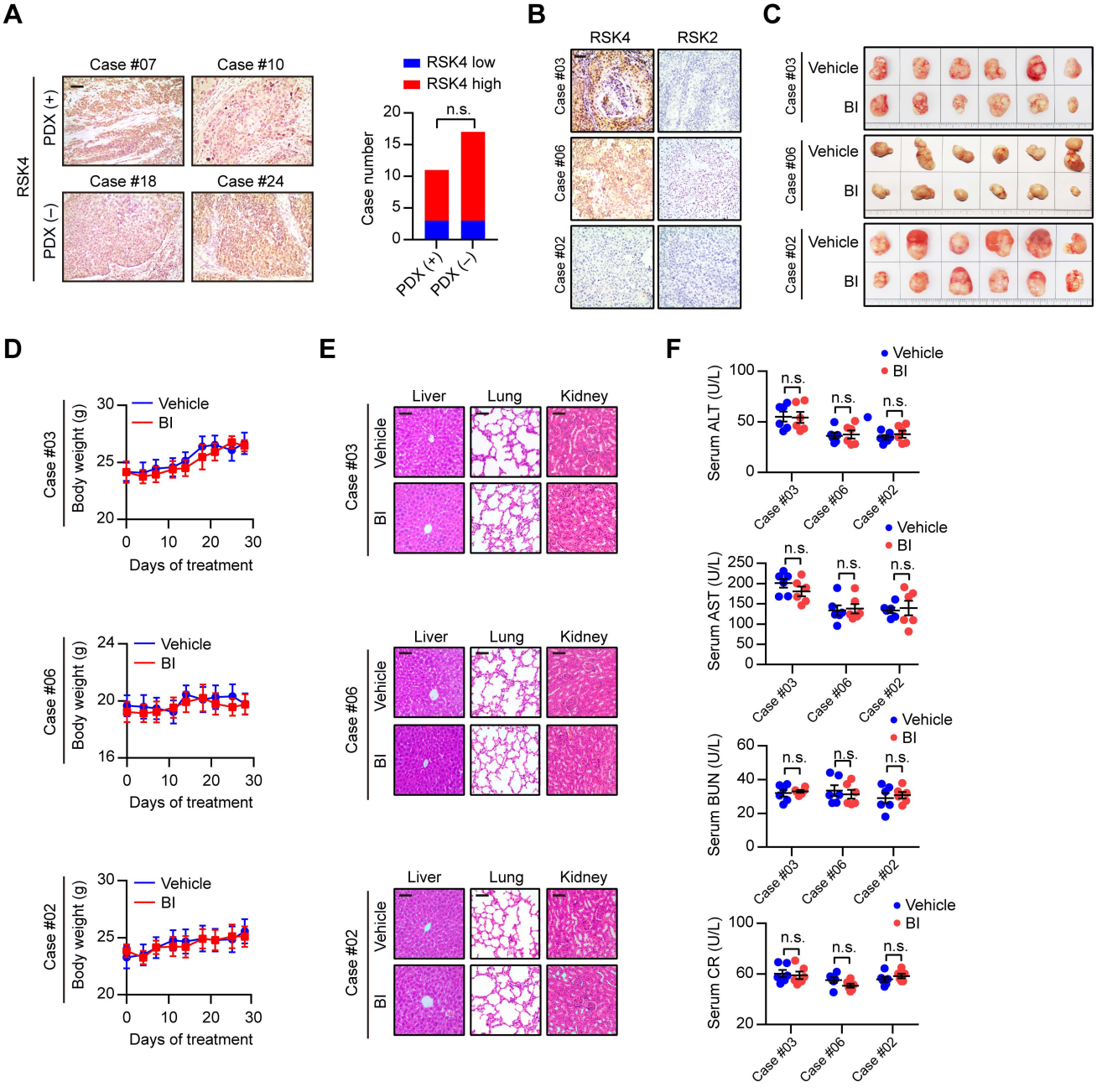

Supplementary Figure 7. Therapeutic effect of BI-D1870 on patient-derived xenografts. (A) Representative immunohistochemical (IHC) staining images of RSK4 in patient-derived xenograft (PDX) successful and unsuccessful models of ESCC tumors. Histograms showing the number of tumors with low or high expression of RSK4 in PDX successful and unsuccessful models. Scale bars, 100 μm. (B) Representative IHC staining images of RSK4 and RSK2 in three PDX models. Scale bars, 100 μm. (C) Representative images of tumor masses from three PDX models treated with BI-D1870 (50 mg/kg per day, intraperitoneal injection) or the vehicle. (D-F) Body weight growth curves (D); representative H&E images of the liver, lung and kidney of mice (E); and the results of serological examinations of alanine transaminase (ALT), aspartate amino transferase (AST), blood urea nitrogen (BUN) and creatinine (Cr) (F) from three PDX models with the indicated treatments are shown (6 mice each). Scale bars, 100 μm. n.s., not significant. Data are representative of means ± SD. Differences were tested using Chi-square test (A) and unpaired 2-sided Student's t test (D, F).

Supplementary Figure 8

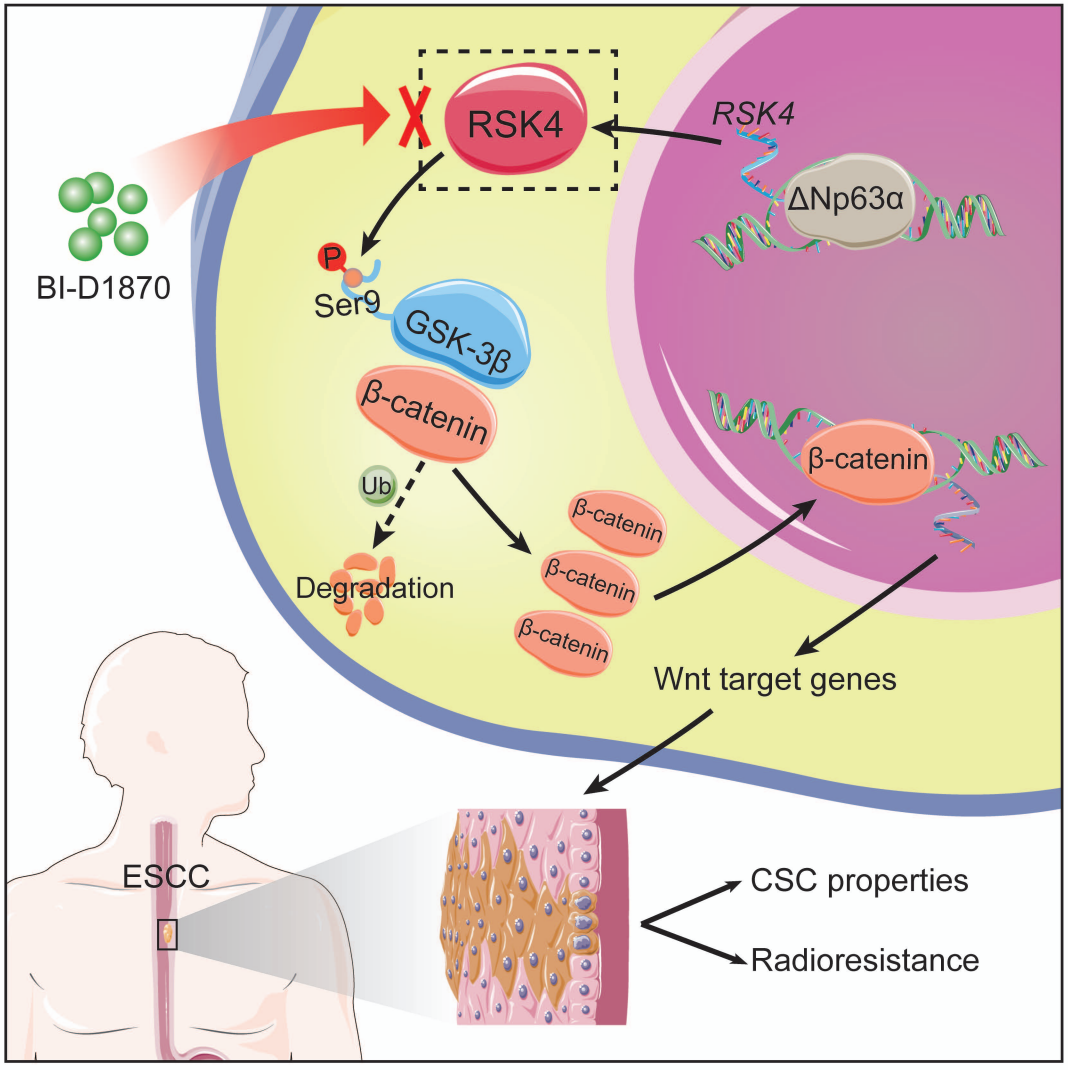

Supplementary Figure 8. Schematic model. In esophageal squamous cell carcinoma (ESCC), overexpression of RSK4 transcriptionally induced by ΔNp63α leads to the phosphorylation of GSK-3β Ser9 and stabilization of β-catenin. Accumulated β-catenin in the cytoplasm translocates into the nucleus to promote the expression of Wnt target genes, which facilitates ESCC CSC properties and radioresistance. Disrupting the RSK4 pathway with BI-D1870 can effectively suppress reduce CSC properties and improve radiosensitivity.

Supplementary Table 1. The information of multiple normal and tumor tissues microarray

Position	Normal tissues	n	Tumors	n
Ⅰ - 1	Stomach	5	Adenocarcinoma	20
Ⅰ - 2	Skin	5	Malignant melanoma	20
Ⅰ - 3	Prostate	5	Adenocarcinoma	20
Ⅰ - 4	Brain	5	Type 1: Astrocytoma Type 2:Glioblastoma	13 7
Ⅰ - 5	Ovary	5	Type 1: Serous papillary adenocarcinoma Type 2: Mucinous adenocarcinoma	12 8
Ⅱ - 1	Breast	5	Invasive ductal carcinoma	20
Ⅱ - 2	Testis	5	Type 1: Seminoma Type 2: Embryonal carcinoma	15 5
Ⅱ - 3	Colon	5	Adenocarcinoma	20
Ⅱ - 4	Bladder	5	Urothelial carcinoma	20
Ⅱ - 5	Uterus	5	Endometrioid adenocarcinoma	20
Ⅲ - 1	Thyroid	5	Type 1: Papillary carcinoma Type 2: Follicular carcinoma	10 10
Ⅲ - 2	Lung	5	Type 1: Squamous cell carcinoma Type 2: Adenocarcinoma	10 10
Ⅲ - 3	Head and neck	5	Squamous cell carcinoma	20
Ⅲ - 4	Lymph node	5	Type 1: Hodgkin's disease Type 2: Diffuse B cell lymphoma	10 10
Ⅲ - 5	Soft tissue	5	Type 1: Fibrosarcoma Type 2: Liposarcoma	10 10
Ⅳ-1	Liver	5	Hepatocellular carcinoma	20
Ⅳ-2	Pancreas	5	Adenocarcinoma	20
Ⅳ-3	Kidney	5	Clear cell carcinoma	20
Ⅳ-4	Cervix	5	Squamous cell carcinoma	20
Ⅳ-5	Esophagus	5	Type 1: Squamous cell carcinoma Type 2: Adenocarcinoma	10 10

Supplementary Table 2. Crosstabulated of RSK4 immunostaining vs clinicalpathological features of ESCC cases in Xijing cohort

Features (n)	RSK4		*P* value
	Positive (n, %)	Negative (n, %)	
Gender			0.482
Male (171)	84 (49.1%)	87 (50.9%)	
Female (44)	19 (43.2%)	25 (56.8%)	
Age (years)			0.840
⩾60 (107)	52 (48.6%)	55 (51.4%)	
＜60 (108)	51 (47.2%)	57 (52.8%)	
Tumour size (cm)			0.627
＞3.0 (106)	49 (46.2%)	57 (53.8%)	
⩽3.0 (109)	54 (49.5%)	55 (50.5%)	
Gross type			0.967
Ulcerative type (113)	54 (47.8%)	59 (52.2%)	
Medullary type (23)	12 (52.2%)	11 (47.8%)	
Constritive type (48)	23 (47.9%)	25 (52.1%)	
Fungating type (31)	14 (45.2%)	17 (54.8%)	
pTNM stage			0.934
Ⅰ-Ⅱ (105)	50 (47.6%)	55 (52.4%)	
Ⅲ-Ⅳ (110)	53 (48.2%)	57 (51.8%)	
Grade			0.731
1 (107)	50 (46.7%)	57 (53.3%)	
2-3 (108)	53 (49.1%)	55 (50.9%)	
T stage			0.580
1-2 (75)	34 (45.3%)	41 (54.7%)	
3-4 (140)	69 (49.3%)	71 (50.7%)	
N stage			**0.015**
0 (102)	40 (39.2%)	62 (60.8%)	
1-3 (113)	63 (55.8%)	50 (44.2%)	
Vascular invasion (CD31)			**0.030**
Yes (84)	48 (57.1%)	36 (42.9%)	
No (131)	55 (42.0%)	76 (58.0%)	
Nerve invasion (S-100)			0.169
Yes (96)	51 (53.1%)	45 (46.9%)	
No (119)	52 (43.7%)	67 (56.3%)	

NOTE. Bold values indicate statistical significance.

Abbreviations: ESCC, esophageal squamous cell carcinoma; pTNM, UICC pathological TNM classification for ESCC (8th edition); T, tumor; N, lymph node.

Supplementary Table 3. Multivariate Cox analysis of overall survival and progression-free survival of ESCC cases in Xijing cohort with follow-up information

Features	Overall Survival		Progression-free survival	
	HR (95% CI)	*P* value	HR (95% CI)	*P* value
Gender (male vs female)	1.193 (0.651-2.186)	0.568	1.083 (0.607-1.932)	0.788
Age (＞60 vs ≤60 years)	0.872 (0.537-1.417)	0.581	0.829 (0.520-1.321)	0.43
Tumour size (＞3 vs ≤3cm)	1.435 (0.851-2.420)	0.175	1.536 (0.930-2.537)	0.094
Gross type	0.993 (0.807-1.222)	0.950	0.986 (0.807-1.206)	0.893
pTNM stage (Ⅲ/Ⅳ vs Ⅰ/Ⅱ)	1.464 (0.622-3.446)	0.383	1.085 (0.496-2.376)	0.838
Grade (2/3 vs 1)	1.025 (0.618-1.698)	0.924	1.107 (0.684-1.791)	0.678
T stage (3/4 vs 1/2)□	2.152 (1.030-4.497)	**0.041**	2.980 (1.469-6.044)	**0.002**
N stage (≥1 vs 0)	1.009 (0.464-2.192)	0.983	1.024 (0.499-2.102)	0.948
Vascular invasion	1.637 (0.921-2.908)	0.093	1.784 (1.024-3.105)	**0.041**
Nerve invasion	0.685 (0.392-1.198)	0.185	0.683 (0.404-1.155)	0.155
RSK4 (high vs low)	2.972 (1.736-5.090)	**0.001**	2.399 (1.442-3.992)	**0.001**

NOTE. Bold values indicate statistical significance.

Abbreviations: ESCC, esophageal squamous cell carcinoma; HR, hazard ratio; 95% CI, 95% confidential interval; pTNM, UICC pathological TNM classification for ESCC (8th edition); T, tumor; N, lymph node.

Supplementary Table 4. Mitogen-activated protein kinase (MAPK) pathway phosphor-antibody microarray map

	A	B	C	D	E	F	G	H
1	POS	POS	NEG	NEG	p-AKT (S473)	p-CREB (S133)	p-ERK1 (T202/Y204) p-ERK2 (Y185/Y187)	p-GSK-3α (S21)
2								
3	p-GSK-3β (S9)	p-HSP27 (S82)	p-JNK (T183)	p-MEK (S217/S221)	p-MKK3 (S189)	p-MKK6 (S207)	p-MSK2 (S360)	p-mTOR (S2448)
4								
5	p-p38 (T180/Y182)	p-p53 (S15)	p-p70S6K (T421/S424)	p-RSK1 (S380)	p-RSK2 (S386)	NEG	NEG	POS
6								

Abbreviations: POS, positive control spot; NEG, negative control spot.

Supplementary Table 5. Crosstabulated of p-GSK-3β immunostaining vs clinicalpathological features of ESCC cases in Xijing cohort

Features (n)	p-GSK-3β		*P* value
	Positive (n, %)	Negative (n, %)	
Gender			0.972
Male (171)	85 (49.7%)	86 (50.3%)	
Female (44)	22 (50.0%)	22 (50.0%)	
Age (years)			0.945
⩾60 (107)	53 (49.5%)	54 (50.5%)	
＜60 (108)	54 (50.0%)	54 (50.0%)	
Tumour size (cm)			0.306
＞3.0 (106)	49 (46.2%)	57 (53.8%)	
⩽3.0 (109)	58 (53.2%)	51 (46.8%)	
Gross type			0.642
Ulcerative type (113)	54 (47.8%)	59 (52.2%)	
Medullary type (23)	14 (60.9%)	9 (39.1%)	
Constritive type (48)	25 (52.1%)	23 (47.9%)	
Fungating type (31)	14 (45.2%)	17 (54.8%)	
pTNM stage			0.538
Ⅰ - Ⅱ (105)	50 (47.6%)	55 (52.4%)	
Ⅲ-Ⅳ (110)	57 (51.8%)	53 (48.2%)	
Grade			0.306
1 (107)	57 (53.3%)	50 (46.7%)	
2-3 (108)	50 (46.3%)	58 (53.7%)	
T stage			0.926
1-2 (75)	37 (49.3%)	38 (50.7%)	
3-4 (140)	70 (50.0%)	70 (50.0%)	
N stage			**0.017**
0 (102)	42 (41.2%)	60 (58.8%)	
1-3 (113)	65 (57.5%)	48 (42.5%)	
Vascular invasion (CD31)			**0.044**
Yes (84)	49 (58.3%)	35 (41.7%)	
No (131)	58 (44.3%)	73 (55.7%)	
Nerve invasion (S-100)			0.446
Yes (96)	45 (46.9%)	51 (53.1%)	
No (119)	62 (52.1%)	57 (47.9%)	

NOTE. Bold values indicate statistical significance.

Abbreviations: ESCC, esophageal squamous cell carcinoma; pTNM, UICC pathological TNM classification for ESCC (8th edition); T, tumor; N, lymph node.

Supplementary Table 6. Antibody information used in immunohistochemistry and western blot

Protein	Application	Origin	Dilution
RSK4	IHC & WB	HPA003904, Sigma-Aldrich	1:50 & 1:200
ΔNp63	IHC	RAB-0666, MXB Biotechnologies	Ready-to-use
ΔNp63	WB	ABS552, Millipore	1:500
p-GSK-3β (Ser9)	IHC & WB	#9323, Cell Signaling Technology	1:50 & 1:1000
RSK1	WB	ab32114, Abcam	1:1000
RSK2	IHC & WB	#5528, Cell Signaling Technology	1:500 & 1:1000
RSK3	WB	14446-1-AP, Proteintech Group	1:1000
Ki-67	IHC	MAB-0672, MXB Biotechnologies	Ready-to-use
γ-H2AX	IHC & WB	#9718, Cell Signaling Technology	1:400 & 1:1000
ALDH1	IHC	ab52492, Abcam	1:100
CD90	IHC	ab133350, Abcam	1:100
β-actin	WB	CW0096, CWBiotech	1:1000
p27 KIP1	WB	25614-1-AP, Proteintech Group	1:2000
p-p27 KIP1 (Ser10)	WB	ab62364, Abcam	1:1000
eIF4B	WB	ab68474, Abcam	1:2000
p-eIF4B (Ser422)	WB	#3591, Cell Signaling Technology	1:1000
HSP27	WB	ab109376, Abcam	1:1000
p-HSP27 (Ser78)	WB	ab32501, Abcam	1:2000
CREB	WB	ab32515, Abcam	1:1000
p-CREB (Ser133)	WB	ab32096, Abcam	1:3000
c-Fos	WB	#4384, Cell Signaling Technology	1:1000
p-c-Fos (Ser32)	WB	#5348, Cell Signaling Technology	1:1000
Histone H3	WB	ab176842, Abcam	1:1000
p-Histone H3 (Ser10)	WB	ab14955, Abcam	1:500
NANOG	WB	#4903, Cell Signaling Technology	1:1000
SOX2	WB	#3579, Cell Signaling Technology	1:1000
BMI-1	WB	#6964, Cell Signaling Technology	1:1000
OCT4	WB	#2840, Cell Signaling Technology	1:1000
CD271	WB	55014-1-AP, Proteintech Group	1:1000
ABCG2	WB	10051-1-AP, Proteintech Group	1:500
β-catenin	WB	#8480, Cell Signaling Technology	1:1000
p-β-catenin (Ser33/37/Thr41)	WB	#9561, Cell Signaling Technology	1:1000
GSK-3β	WB	#12456, Cell Signaling Technology	1:1000
TCF1	WB	#2203, Cell Signaling Technology	1:1000
MYC	WB	#5605, Cell Signaling Technology	1:1000
CD44	WB	60224-1-lg, Proteintech Group	1:1000
Caspase-3	WB	#9665, Cell Signaling Technology	1:1000
Cleaved Caspase-3	IHC & WB	#9664, Cell Signaling Technology	1:500 & 1:1000
PARP	WB	#9532, Cell Signaling Technology	1:1000
Cleaved PARP	WB	#9546, Cell Signaling Technology	1:1000
β-Tubulin	WB	KM9003, Sungene Biotech	1:3000
Lamin B	WB	12987-1-AP, Proteintech Group	1:3000
HA-Tag	WB	#3724, Cell Signaling Technology	1:1000
Flag-Tag	WB	#14793, Cell Signaling Technology	1:1000
His-Tag	WB	#2366, Cell Signaling Technology	1:1000
V5-Tag	WB	#13202, Cell Signaling Technology	1:1000
ATM	WB	#2873, Cell Signaling Technology	1:1000
p-ATM (Ser1981)	WB	#13050, Cell Signaling Technology	1:1000
CHK2	WB	#6334, Cell Signaling Technology	1:1000
p-CHK2 (Thr68)	WB	#2197, Cell Signaling Technology	1:1000
PLK1	WB	#4513, Cell Signaling Technology	1:1000
Cdc25C	WB	ab32444, Abcam	1:2000
p-Cdc25C (Ser198)	WB	#9529, Cell Signaling Technology	1:1000
Cyclin B1	WB	ab72, Abcam	1:1000
p-Cyclin B1 (Ser147)	WB	ab60986, Abcam	1:500
Aurora B	WB	#3094, Cell Signaling Technology	1:1000
NPM1	WB	ab52644, Abcam	1:2000
p-NPM1 (Ser125)	WB	ab109546, Abcam	1:1000

Abbreviations: IHC, immunohistochemistry; WB, western blot.

Supplementary Table 7. Primer sequences used in the study

Primer name	Sequence (5'-3')
Primers for real-time PCR:	
RSK1 sense	CACCTGTATGCTATGAAGGTGCTG
RSK1 antisense	TAGAGCTTGCCCTCGGTCTG
RSK2 sense	GGCCAGTGCTGTCCTGTTCA
RSK2 antisense	CCGGATTACCAGATTCATCCACATA
RSK3 sense	CTGCACAAAGTCCCAGTTCACC
RSK3 antisense	ATGCACACATCGCTTGCACA
RSK4 sense	TGCTCAAGGTTCTTGGTCAG
RSK4 antisense	TTTGTCCGAACTCTGTCTCG
TAp63 sense	TGTATCCGCATGCAGGACT
TAp63 antisense	CTGTGTTATAGGGACTGGTGGAC
ΔNp63 sense	GAAAACAATGCCCAGACTCAA
ΔNp63 antisense	TGCGCGTGGTCTGTGTTA
GAPDH sense	GCACCGTCAAGGCTGAGAAC
GAPDH antisense	TGGTGAAGACGCCAGTGGA
p63α sense	GAGGTTGGGCTGTTCATCAT
p63α antisense	AGGAGATGAGAAGGGGAGGA
p63β sense	AACGCCCTCACTCCTACAAC
p63β antisense	CAGACTTGCCAGATCCTGA
p63γ sense	ACGAAGATCCCCAGATGATG
p63γ antisense	GCTCCACAAGCTCATTCCTG
NANOG sense	CATGAGTGTGGATCCAGCTTG
NANOG antisense	CCTGAATAAGCAGATCCATGG
SOX2 sense	CAAGATGCACAACTCGGAGA
SOX2 antisense	GCTTAGCCTCGTCGATGAAC
OCT4 sense	AGTGAGAGGCAACCTGGAGA
OCT4 antisense	ACACTCGGACCACATCCTTC
CD90 sense	CGCTCTCCTGCTAACAGTCTT
CD90 antisense	CAGGCTGAACTCGTACTGGA
CD271 sense	ACGGCTACTACCAGGATGAG
CD271 antisense	TGGCCTCGTCGGAATACGTG
BMI-1 sense	TCGTTGTTCGATGCATTTCT
BMI-1 antisense	CTTTCATTGTCTTTTCCGCC
ABCG2 sense	TGGTGTTTCCTTGTGACACTG
ABCG2 antisense	TGAGCCTTTGGTTAAGACCG
Primers for shRNA:	
shRSK4 #1	GATCCGGGTAAATGGTCTTAAAATGTCAAGAGCATTTTAAGACCAT TTACCTTTTTTGGAATT
shRSK4 #2	GATCCGGCTCCTGAAGTAGTAAATATCAAGAGTATTTACTACTTCAG GAGCTTTTTTGGAATT
shΔNp63 #1	GATCCGTGCCCAGACTCAATTTAGTTCAAGAGACTAAATTGAGTCTA AACTTTTTTTGGAATT
shΔNp63 #2	GATCCGGGCCGTGAGACTTATGAAATCAAGAGTTTCATAAGTCTCA CGGCCTTTTTTGGAATT
Primers for RSK4 promoter construct:	
RSK4 promoter sense	AGTATCGAAATGGGCGTGGTT
RSK4 promoter antisense	GGCGGCAGGATTCTCAAAAA

Supplementary methods

Patients and specimens. Fresh human ESCC tissues and adjacent noncancerous normal tissues for real-time PCR and Western blot analyses (n = 30) were collected from patients at Xijing Hospital between 2013 and 2014. A total of 215 consecutive patients (Xijing cohort) who underwent radical resection for ESCC between 2010 and 2012 were identified from the pathology archives of Xijing Hospital. The patients' charts were reviewed, and those who had pre-operative radiation or chemotherapy, or were immunocompromised, were excluded. A total of 148 consecutive patients (Radiotherapy cohort) treated with definitive radiotherapy between 2011 and 2016 were selected from the Department of Radiotherapy, Xijing Hospital. All of the patients enrolled received the same dose of radiation (50.4 Gy).

Real-time PCR. Total RNA was extracted using TRIzol reagent (Invitrogen, Carlsbad, CA, USA) and identified using reverse transcription-PCR and a SYBR Green II kit (Takara, Shiga-ken, Japan). The mRNA expression levels of the target genes were normalized to those of the *GAPDH* gene. The primer pairs used in this study are listed in **Supplementary Table 7**.

Western blot analysis. For Western blot analysis, total protein from tissue or cells was obtained using RIPA lysis buffer (20 mM Tris-HCl pH 7.5, 150 mM NaCl, 1 mM EDTA, 1% Nonidet P-40, 0.5% sodium deoxycholate and 0.1% SDS) containing a protease inhibitor (CW2200, CWBiotech, Beijing, China) and phosphatase inhibitor (CW2383, CWBiotech, Beijing, China). For nuclear protein extraction, the assays were performed according to the manufacturer's instructions for the Qproteome Cell Compartment Kit

(Qiagen, Hilden, Germany). After determining the protein concentration using the Pierce BCA Protein Assay Kit (23225, Thermo Fisher Scientific, Waltham, MA, USA), equal amounts of protein were separated via SDS–PAGE using a 10% SDS–PAGE gel and then were transferred to PVDF membranes (Millipore, Billerica, MA, USA). After blocking with 5% skim milk in TBST, the membranes were incubated with the indicated primary antibodies overnight at 4°C. Antibody information is shown in **Supplementary Table 6**. Then, the membranes were incubated with secondary HRP-conjugated antibodies for 1 h at room temperature after washing. Blots were developed using the ChemiDoc-It Imaging System (UVP, Upland, CA, USA) according to the manufacturer's instructions. Protein expression levels were quantified with ImageJ software (National Institutes of Health, Bethesda, MD, USA) and normalized to the levels of β-actin.

Lentiviral production and transduction. The RSK4 ORF sequence (NM_014496.4) and ΔNp63α (NM_001114980.1) were PCR-amplified using specific primers and cloned into the lentiviral expression vector pEZ-Lv201 to develop RSK4 and ΔNp63α recombinant plasmids (GeneCopoeia, Rockville, MD, USA). To construct shRNAs of RSK4 and ΔNp63 into the shRNA expression vector psi-LVRU6GP (GeneCopoeia, Rockville, MD, USA), the target sequences **(Supplementary Table 7)** were synthesized and inserted into the vector. The shRNA with a non-targeting sequence was used as a negative control. The constructed vectors were transfected into 293T cells to produce viruses. Cells including ECA109, EC9706, TE10 and TE11 were infected with concentrated viruses, and the supernatant was replaced with complete culture media

after 24 h, followed by selection with puromycin.

Caspase-3 activity assay. Caspase-3 activities in cell culture were detected 24 h after IR using the Caspase 3 Activity Assay Kit (C1115, Beyotime Biotechnology, Shanghai, China) according to the manufacturer's instructions. Ac-DEVD-pNA (2 mM) was added into cell lysis detection solution, and the absorbance at 405 nm was measured after incubation for 2 h at 37°C to calculate the caspase-3 activity.

Tumor sphere-forming assay. One thousand cells were seeded into ultra-low attachment 6-well plates in serum-free DMEM/F12 medium (Gibco, Carlsbad, CA, USA) supplemented with 2% B27 (Invitrogen), 10 ng/mL epidermal growth factor (EGF, Invitrogen), and 10 ng/mL basic fibroblast growth factor (bFGF, Invitrogen). The medium was changed every three days until tumor sphere formation was observed (approximately 2 weeks). The sphere diameters and morphology were examined by a light microscopy (IX53, Olympus, Tokyo, Japan).

Flow cytometry analysis. ESCC cells were incubated with PE-conjugated anti-CD90 (Biolegend, San Diego, CA, USA) and PE-conjugated anti-CD271 (Biolegend, San Diego, CA, USA) followed by flow cytometry analysis using a CytoFLEX flow cytometer (Beckman Coulter, Brea, CA, USA). ALDH activity was measured by using the ALDEFLUOR™ Detection Kit (01700, StemCell Technology) according to the manufacturer’s instructions, and data was acquired on a CytoFLEX flow cytometer (Beckman Coulter, Brea, CA, USA).

Magnetic sorting. ESCC cell lines were labeled with biotin-conjugated anti-CD90 (Biolegend, San Diego, CA, USA) or biotin-conjugated anti-CD271 (BD Biosciences,

Franklin Lakes, NJ, USA), followed by incubation with goat anti-mouse IgG microbeads (Miltenyi Biotec, Germany). The cells were then magnetically sorted on MACS LS columns (Miltenyi Biotec, Germany) according to the manufacturer's instructions.

Dual-luciferase reporter assay. Analysis of the promoter region of RSK4 was performed using MatInspector Professional software (Genomatix Inc., Ann Arbor, MI, USA) on a region 1000 bp upstream of the transcription start site of the human RSK4 gene. To validate the p63 binding sites in the RSK4 promoter, RSK4 promoter reporters with the wild-type (pEZX-PG04.1-WT) or deletion-mutated p63 binding sites (pEZX-PG04.1-MUT) were constructed (GeneCopoeia, Rockville, MD, USA). HEK293T cells were cotransfected with 300 ng of the ΔNp63α plasmid (Addgene, Cambridge, MA, USA), 100 ng of the RSK4 promoter reporter plasmid, and 2 ng of the pRL-cytomegalovirus vector plasmid using Lipofectamine 2000 (Invitrogen). Luciferase activity assays were performed 48 h after the transfections using the Dual-Luciferase Reporter Assay System (GeneCopoeia, Rockville, MD, USA) on a Lumat LB 9507 Luminometer (Promega) per the manufacturer's recommendation. Renilla luciferase activity was utilized to normalize the transfection efficiency.

Chromatin immunoprecipitation assay. After cells were transfected with the appropriate plasmids, a chromatin immunoprecipitation (ChIP) assay was performed using the EZ-ChIP^{TM} Kit (17-371; Millipore, Billerica, MA). The following antibodies were utilized to immunoprecipitate crosslinked protein-DNA complexes: rabbit anti-p63 (sc-8343 from Santa Cruz Biotechnology) and normal rabbit IgG (sc-2027 from

Santa Cruz Biotechnology). The immunoprecipitated DNA was purified for PCR analyses with primers specific for the putative binding sites within the promoter of RSK4 **(Supplementary Table 7)**.

Immunofluorescence. Tumor cells were fixed with 4% paraformaldehyde, permeabilized with 0.1% Triton X-100 for 10 min, and then blocked with 2% BSA. The cells were incubated with the primary antibodies against β-catenin (1:100, 8480 from Cell Signaling Technology), GSK-3β (1:400, 12456 from Cell Signaling Technology), RSK4 (1:100, sc-100424 from Santa Cruz Biotechnology) or γ-H2AX (1:200, 9718 from Cell Signaling Technology) overnight at 4°C, followed by fluorophore-conjugated secondary antibody (goat anti-mouse IgG, FITC-conjugated, CWBiotech; goat anti-rabbit IgG, TRITC-conjugated, CWBiotech). Images were acquired using a confocal laser scanning microscopy FluoView FV1000 (Olympus, Tokyo, Japan).

Glutathione S-transferase (GST) pulldown assay. GST and GST-RSK4 proteins were purchased from Sino Biological (11213-HNAE and 10147-H09B, Beijing, China). GST fusion proteins were incubated with glutathione agarose (Pierce, Rockford, IL, USA) followed by the addition of cell lysates or His-GSK-3β protein according to the manufacturer's instructions. Unbound proteins were removed after several washes. The proteins were eluted by boiling in loading buffer for SDS-PAGE and immunoblotting.

Immunoprecipitation assay. Cells were lysed in ice-cold IP buffer (20 mM Tris-HCl pH 7.4, 150 mM NaCl, 1 mM EDTA and 1% Triton X-100) containing protease inhibitor (CW2200, CWBiotech) and phosphatase inhibitor (CW2383, CWBiotech). The lysates were centrifuged at 12,000 g for 15 min and then collected and incubated

with the indicated antibodies including GSK-3β (12456 from Cell Signaling Technology), Flag-Tag (14793 from Cell Signaling Technology), RSK4 (sc-100424 from Santa Cruz Biotechnology), HA-Tag (2367 from Cell Signaling Technology) or His-Tag (2366 from Cell Signaling Technology) and Protein A/G Agarose beads (sc-2003, Santa Cruz Biotechnology) overnight at 4°C. After washing three times in cold immunoprecipitation buffer, the immunocomplexes were collected and subjected to immunoblotting.

Plasmid construction. HA-GSK-3β, Flag-RSK4 and His-β-catenin plasmids were purchased from Sino Biological Company (HG10044-CY, HG10147-NF and HG11279-CH, Beijing, China). Control-Flag vector was purchased from Sigma. V5-ubiquitin and Control-V5 plasmids were preserved in our in-house construct bank. The truncations of CTKD+KIM (amino acids 331-745 aa), NTKD+CTKD (amino acids 1–683), and NTKD (amino acids 1–330) of RSK4 were constructed in the pCMV3-Flag vector using standard molecular biology techniques. GSK-3β S9A and S9D mutants were constructed in the pCMV3-HA vector with the QuikChange Mutagenesis Kit (Stratagene, Inc., La Jolla, CA, USA). All constructs used in our study have been thoroughly sequenced.

Cell viability and apoptosis assay. In vitro proliferation of ESCC cells was measured using Cell Counting Kit-8 (7sea Biotech, Shanghai, China). According to the manufacturer's instructions, cells were seeded in 96-well plates at 2×10^3 per well in a final volume of 100 μL and cultured at 37°C to obtain viable cells. Cell apoptosis was evaluated using the Annexin V-FITC Apoptosis Detection Kit (7sea Biotech, Shanghai,

China) on a CytoFLEX flow cytometer (Beckman Coulter, Brea, CA, USA) based on the manufacturer's guidance.

Intermolecular interaction between BI-D1870 and the modeled RSK4 structure. The N-terminal kinase domain (NTKD) of the RSK2 protein (PDB ID: 5D9K) was used as the template to construct the NTKD model of RSK4 (sequence identity: 91%). Homology modeling was performed using Maestro (Schrödinger, LLC, NY, USA) with default settings. The Ramachandran plot and verify-3D test were performed using Procheck (Yale University, CT, USA) to evaluate the reliability of the model. Using Maestro, BI-D1870 was prepared through the LigPrep module and docked into the ATP binding site of RSK4 NTKD prepared in the Protein Preparation Wizard by Glide. Finally, the top-ranked conformations of BI-D1870 by GScore were selected for further binding mode analysis.

Terminal deoxynucleotidyl transferase-mediated dUTP labeling (TUNEL) assay. Apoptotic cells in serial sections of xenograft tumors were determined by TUNEL assay using the *In Situ* Cell Death Detection Kit POD (Roche Diagnostics, Mannheim, Germany), which quantitatively determines DNA fragmentation visualized with 3,3'-diaminobenzidine tetrahydrochloride, according to the manufacturer's instructions. The presence of strong nuclear staining indicated apoptotic cells.

Comet assay. The alkaline comet assay was undertaken using a COMET assay kit (Bio-Techne, Minneapolis, MN, USA) according to the manufacturer's instructions. At least 50 cells were captured using a fluorescence microscope (Leica Microsystems, Wetzlar, Germany) in each sample. The percentage of DNA in the tail was analyzed by CASP

software (http://casplab.com).

Xenograft tumor-formation assay. For tumor formation with a gradient dilution of ESCC cells, BALB/c nude mice (5 mice per group) were subcutaneously injected with 0.2 μL of cell suspension containing various amounts of cells (1×10^2, 1×10^3, 1×10^4, 1×10^5 cancer cells) into the back flank. Tumor size was measured every 5 days until 60 days after injection. Stem cell frequency was calculated using extreme limiting dilution analysis (http://bioinf.wehi.edu.au/software/elda/). To evaluate changes in tumor volume after each therapeutic regimen, when tumors had grown to a volume of 200 mm^3, mice were randomized into four groups (5 mice per group): Vehicle; Vehicle+IR (ionizing radiation); BI-D1870; and BI-D1870+IR. A total of 10 Gy (5 Gy×2 times) was delivered to animals restrained in custom lead jigs for localized IR treatment at the 7^{th} and 14^{th} day after dividing groups. In our animal experiments, we used hypofractionation radiotherapy (5 Gy×2 times) for treatment, while in clinical applications, the most commonly prescribed treatment is conventional fractionation radiotherapy (1.8-2.2 Gy per fraction for five fractions in a week). BI-D1870 was administered at 50 mg/kg via intraperitoneal injection daily. Animals were raised for 20 days, and tumor volume was measured every 5 days and calculated by length × $width^2\times0.5$. All animals were housed in a virus-free facility and maintained in a temperature and light (12 h light/dark cycle) controlled animal facility.

Phosphor-antibody array. Analysis of the phosphorylation status of several kinases was performed using the MAPK Pathway Phosphorylation Array Kit (AAH-MAPK-1, RayBiotech, Norcross, GA, USA) according to the manufacturer's instructions

(Supplementary Table 4). Briefly, cells were washed in PBS and incubated with Lysis Buffer for 30 min at 4°C. Cell debris was removed by centrifugation at 14,000 g for 10 min, and the protein concentration was assessed by a BCA Protein Assay (Thermo Fisher Scientific, Waltham, MA, USA). After blocking in Blocking Buffer for 30 min at room temperature, each membrane was incubated with cell lysate overnight at 4°C. Membranes were then washed with Wash Buffer and incubated with diluted Detection Antibody Cocktail. Membranes were then incubated with Detection Buffer for 2 min and tested using a ChemiDoc-It Imaging System (UVP, Upland, CA, USA) according to the manufacturer's instructions. Densitometry analysis was performed using ImageJ software (National Institutes of Health, Bethesda, MD, USA) according to the manufacturer's instructions.